Reprinted from January 1981, Vol. 103, Journal of Lubrication Technology

N. Maw
Department of Mechanical Engineering,
Sunderland Polytechnic,
Sunderland, England

J. R. Barber

J. N. Fawcett
Department of Mechanical Engineering,
University of Newcastle-upon-Tyne,
Newcastle-upon-Tyne, England

The Role of Elastic Tangential Compliance in Oblique Impact

An extension of the Hertz theory of impact to the oblique impact of elastic bodies with circular contact is outlined. The tangential compliance of the contact surface under the action of Coulomb friction is shown to have a significant effect on the rebound angles, if the local angle of incidence does not greatly exceed the angle of friction. Experiments are described in which the trajectory of a moving body is measured before and after impact with a fixed block of similar material. Results obtained using both steel and rubber show good agreement with the theoretical values.

Introduction

The classical theory of impact of two elastic bodies is based on the principles of conservation of energy and momentum and it predicts rebound velocities for given incident velocities without detailed consideration of local elastic deformation.

In the case of oblique impact two conditions can be distinguished: (i) sliding and (ii) rolling of one body over the other. Sliding will generally occur at the start of the impact, but an opposing frictional force will be set up tending to reduce the sliding velocity. If this velocity reaches zero during the impact, sliding gives way to rolling and the frictional force falls instantaneously to zero. Once rolling is established, it persists to the end of the impact.

A theory of colinear impact including the elastic deformations of the bodies was developed by Hertz (1892) from his solution to the problem of elastic contact. This theory enables predictions to be made about (for example) the stress and displacement fields in the bodies and the duration of the impact, some of which have been confirmed experimentally (Lifshitz and Kolsky (1964), Hunter (1957)), but the major conclusions of the classical theory are unchanged. Hertz's theory is quasi-static in the sense that it neglects loss of energy in transmitted stress waves. A justification for this is given by Hunter (1957).

By contrast, it will be demonstrated both theoretically and experimentally in the present paper that, in oblique impact, the elastic deformations of the bodies produce effects which are qualitatively different from those predicted by the classical theory, except in the special case where sliding persists throughout the impact.

A simple demonstration of these effects can be performed by projecting a rubber "superball" with backspin onto a horizontal plane. The ball will rebound backwards and, contrary to the predictions of the classical theory, again with back spin. At the second impact, conditions are therefore much the same as they were at the first except that the directions are reversed. The trajectory of the ball is always towards the locality of the previous impact.

As the bodies respond to friction forces some of the work done in deflecting the bodies tangentially is stored as elastic strain energy in the solids and is recoverable under suitable circumstances. The relative tangential displacements are not necessarily constant over the contact area and it is possible for some regions to be stuck while others are sliding. An example of this is analyzed by Mindlin (1949) for the static case in which two identical spheres are pressed together under a constant normal force and are then subjected to a tangential force. He showed that, even when the tangential load is very small, an annulus of slip is generated at the boundary of contact. If the tangential load is now allowed to increase, the inner radius of this annulus progressively reduces until, when the critical value of friction force is reached, the bodies start to slide. Mindlin described these conditions as "microslip" and "gross-slip," respectively.

Theoretical Background

Conditions during an impact are considerably complicated by the fact that the contact area is continually changing.

Several static contact problems involving varying normal and tangential load were considered by Mindlin and Deresiewicz (1953), who emphasize that the response of the system to current small changes depends upon the whole previous load history. They confined their attention to cases in which the load history is known and fairly simple.

In the impact problem, neither the normal nor the

Contributed by the Lubrication Division of THE AMERICAN SOCIETY OF MECHANICAL ENGINEERS and presented at the Century 2 ASME-ASLE International Lubrication Conference, San Francisco, Calif., August 18-21, 1980. Revised manuscript received by the Lubrication Division, February 26, 1980. Paper No. 80-C2/Lub-22.

tangential forces are known a priori. To achieve a solution, therefore, the impact is imagined to occur over a succession of discrete time increments. Starting from known values of normal and tangential velocity the displacements in a time interval are found. These define the boundary conditions of the instantaneous contact problem and allow changes in normal and tangential forces to be determined from elasticity considerations. The velocity components at the next interval are then found from changes in momentum.

A theory for oblique impact has been developed for the case of a sphere impacting a half-space of similar material[1] but it is applicable to more general cases such as the non-colinear collision of two bodies with spherical surfaces whose centers of mass are situated at their centers of curvature. Examples of these are spheres or symmetrical slices cut from spheres. The following assumptions are made in the derivation.

(i) The contact area is regarded as small compared with the general sizes of the impacting bodies.

(ii) The coefficient of static friction is equal to the coefficient of dynamic friction and remains constant. This is considered reasonable when applied to initial slip on newly cleaned surfaces (reference [8]).

(iii) The material of the impacting bodies behaves in a linearly elastic manner. The series of experiments for normal impact by Lifshitz and Kolsky (1964) supports this assumption.

(iv) The theory follows Hertz in being quasi-static.

(v) The distribution of tangential traction (surface shear stress) is axisymmetric.[2]

The foregoing assumptions imply that the coefficient of restitution is unity, the area of contact remains circular and the normal force is not affected by the tangential force.

Solutions. Two methods of solution have been developed although they are, in principle, equivalent. The first by Maw (1976) uses the general approach of Mindlin and Deresiewicz to solve each of the incremental contact problems throughout the impact. However, with this method, the previous load history of the system has to be continuously available at each step. Consequently, after the nth step, the state is described as the sum of n irreducable components. This places a practical limit on the number of time intervals which can be used.

[1] This requirement is necessary to guarantee uncoupling between normal and tangential effects, a condition which is satisfied more generally (Spence (1968)) if the material properties are such that

$$\frac{\left(\frac{1-2\nu_1}{G_1}\right)-\left(\frac{1-2\nu_2}{G_2}\right)}{\left(\frac{1-\nu_1}{G_1}\right)+\left(\frac{1-\nu_2}{G_2}\right)}=0$$

which includes similar materials or rubber ($\nu_1 = 0.5$) in contact with a rigid surface ($G_2 >> G_1$). ν is Poisson's ratio and G is the modulus of rigidity.

The second method, described by Maw, Barber, and Fawcett (1976) is based upon the premise that the load history only influences the behavior of the system insofar as it defines the net "locked-in" tangential displacement at any instant. The information carried through the procedure is therefore independent of the number of increments used. The potential contact region is divided into a series of equi-spaced concentric annuli. For each step a provisional division into stick and slip regions is assumed and the tangential traction and displacement distribution is determined in all regions. In stick regions the tangential tractions must be below the limits at which slip occurs whereas, in slip regions, the relative incremental displacement must be in the correct sense for the assumed traction. The solution is tested to see whether the assumed division is correct. If the test fails in any region the assumption in that region is changed and a new solution is obtained. Convergence is rapid.

The results from the two methods have been found to agree closely in cases to which both can be applied, but the second method affords a clear computational advantage.

Nondimensional Parameters. The problem can be defined in terms of two nondimensional parameters which apply to all materials, all dimensions and all initial conditions. One of these parameters,

$$\chi=\frac{\left(1-\nu\right)\left(1+\frac{1}{K}^2\right)}{2-\nu} \tag{1}$$

is related to the radius of gyration, $K = (I/_{MR}2)^{1/2}$, I is the moment of inertia, M is the mass and R is the radius of the body impacting the half-space.

The other parameter is the local nondimensional tangential velocity,

$$\psi=\frac{2(1-\nu)}{\mu(2-\nu)}\cdot\frac{V_x}{V_{z1}} \tag{2}$$

where V_{z1} is the initial value of V_z, the normal velocity of the contact patch, and V_x is the corresponding tangential velocity. μ is the coefficient of friction. The parameter ψ is proportional to the ratio of the tangents of the local angle of incidence (measured from the common normal) and the angle of friction.

The range of values of χ occurring in practice is small. A typical value of χ for a solid steel sphere for example is 1.44 while for a rubber disk it is 1.00. No such practical limits are attached to the parameter ψ.

[2] This is exact if the stuck regions are surrounded by slip regions (Mindlin's case) but, in other circumstances, for example, if slip regions are surrounded by stuck regions, the solution for traction distribution contains non-axisymmetric terms. However, the offending terms are small and would contribute little error. The matter is discussed by Maw, Barber, and Fawcett (1976) in some detail.

Nomenclature

ν = Poisson's ratio
G = modulus of rigidity
χ = parameter related to the radius of gyration – featured in equation (1)
ψ = parameter related to the local tangential velocity – featured in equation (2)
Vz = normal velocity of contact patch
Vx = tangential velocity of contact patch
μ = coefficient of friction
F = friction force
P = normal force
M = mass
K_T = tangential stiffness
K_N = normal stiffness
τ = ratio of time lapsed from initial contact to impact duration
$f(r)$ = tangential traction at radius r
$p(r)$ = normal pressure at radius r
b = radius of contact circle
R = radius of spherical surface of body impacting half-space
$Ux(r)$ = elastic displacement due to $f(r)$ in direction of traction
$Uy(r)$ = elastic displacement due to $f(r)$ in tangential direction perpendicular to the traction
θ = polar coordinate measured from positive x axis
C = $\left[\frac{15\ MVz^2{}_1\ (1-\nu)}{16GR^3}\right]^{1/5}$ (see reference [3])

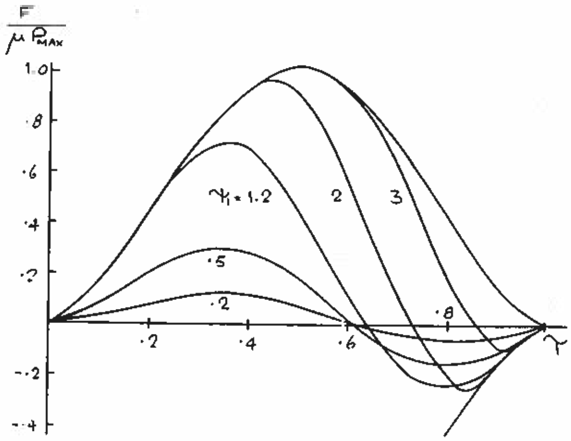

Fig. 1 Nondimensional tangential force, for different angles of incidence, ψ_1, plotted against nondimensional time, τ, for a steel disk ($\nu = 0.28$, $\chi = 1.256$)

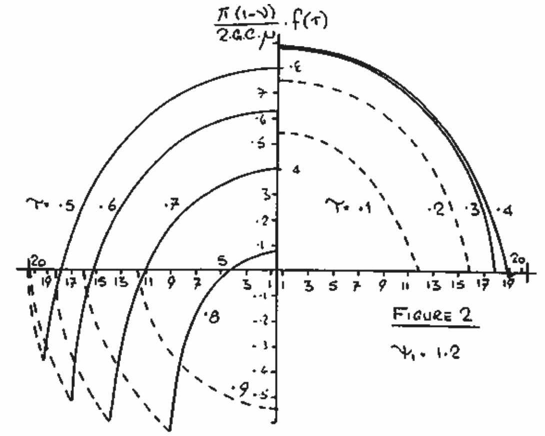

Fig. 2 The radial distribution of nondimensional traction at different intervals, τ, in the cycle. The lines in chaindash show the traction in slip regions.

$$C = \left[\frac{15MV_{Zi}^2(1-\nu)}{16\ GR^3}\right]^{1/5}$$

Theoretical Predictions. The initial conditions of the impact system are characterized by the nondimensional local angle of incidence, ψ_1. Maw, Barber, and Fawcett (1976) have shown that three regimes can exist in a typical impact.

(i) $\psi_1 \leq 1$

For these relatively small angles of incidence the surfaces stick and, as the impact proceeds, new annuli are laid down in such a way that they are free of tangential traction until shortly before maximum compression when microslip commences. However, once the maximum compression is passed and the contact area begins to decrease the interface can no longer sustain the traction and the elastic strain energy commences to dissipate in microslip. An annulus of slip spreads inwards until, eventually, the whole contact area slides, i.e., gross-slip is established.

(ii) $1 < \psi_1 < (4\chi - 1)$

In these intermediate ranges of incidence angles the impact commences in gross-slip. Hence, traction is everywhere a constant proportion, μ, of the normal Hertzian pressure and the relative velocity between the two surfaces decreases because of the friction force. All points in the contact region have the same velocity under conditions of gross-slip (see Appendix) so that when the velocity of sliding reduces to zero, the conditions over the whole of the contact area change instantaneously from gross-slip to complete stick.

The subsequent history of the impact is similar to that described in (i), above. As ψ_1 is increased the slip-stick transition occurs later in the cycle.

(iii) $\psi_1 \geq (4\chi - 1)$

The whole impact now takes place in gross-slip.

Tangential Force. Figure 1 shows the variation of tangential force during the cycle for various values of ψ_1. The forces are plotted nondimensionally so that the envelope of the curves forms the friction boundaries, $\pm \mu P$. The value of χ is fixed at 1.256 corresponding to a solid uniform disk for which $\nu = 0.28$. The surface of the disk is assumed to be spherical, but the influence of the sphericity on the value of χ is neglected. At all angles of incidence the tangential force shows a complete cycle of oscillation with the reversal in direction occurring later as ψ_1 increases. The deformable surfaces can be imagined to act as a spring in the tangential direction. If $\psi_1 = 1.2$ (about 10 deg when $\mu = 0.12$) is taken as a typical case, then at the start of impact, gross-slip occurs in the direction of the initial tangential velocity and the friction force begins to charge the spring with elastic energy. At about 25 percent of the cycle time the surfaces stick but the "spring" still extends. The oscillation follows a normal pattern until toward the end of the cycle, when the end of the spring is moving in the same direction as the disk surface but at a greater speed. Slip, but in the opposite sense to that at the beginning, is re-established and persists for the remainder of the impact.

The cyclic nature of the tangential motion can be appreciated when the problem is linearized in the normal and tangential directions. It is first established that the tangential force

$$F = M\left(1 + \frac{1}{K}{}^2\right)^{-1} \frac{dV_x}{dt} \tag{3}$$

where $M\ (1 + 1/K^2)^{-1}$ is the effective mass of the body referred to the tangential motion of the point of contact. Mindlin (1949) shows that the ratio of the tangential stiffness to the normal stiffness

$$\frac{K_T}{K_N} = \frac{1-\nu}{1-\nu/2} \tag{4}$$

for adhesive contact and a given radius of the contact area.

For a linear system with stiffnesses in this ratio, the ratio of the corresponding natural frequencies would be

$$\frac{\omega_T}{\omega_N} = \left[\left(\frac{1-\nu}{1-\nu/2}\right)\left(1 + \frac{1}{K}{}^2\right)\right]^{1/2} = \sqrt{2\chi} \tag{5}$$

which has a value of 1.58 for the steel disk of Fig. 1. If χ is increased (and hence K is reduced) the natural frequency of tangential vibration increases, but it should be noted that χ cannot vary very much for simple systems.

Tractions. Figure 2 shows the radial traction distribution, $f(r)$, for an angle of incidence $\psi_1 = 1.2$. The horizontal scale divides the radius into 20 equal annuli corresponding to the divisions used in the numerical solution (the twentieth annulus represents the largest zone when the normal force reaches its maximum value).

To show the variation of traction at all radii during the impact, patterns are plotted for ten equal time increments throughout the cycle. The change from gross-slip to complete stick occurs between $\tau = 0.2$ and 0.3. At about 40 percent of

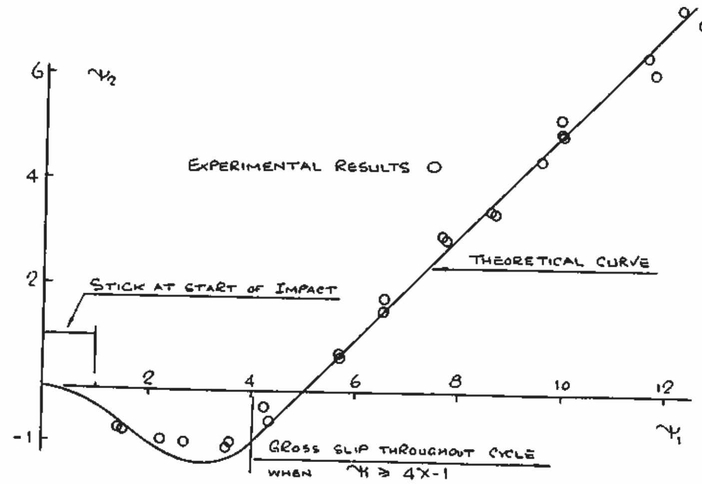

Fig. 3 Nondimensional angles of reflexion, ψ_2, plotted against nondimensional angle of incidence, ψ_1, for a steel disk (ν = 0.28, χ = 1.256)

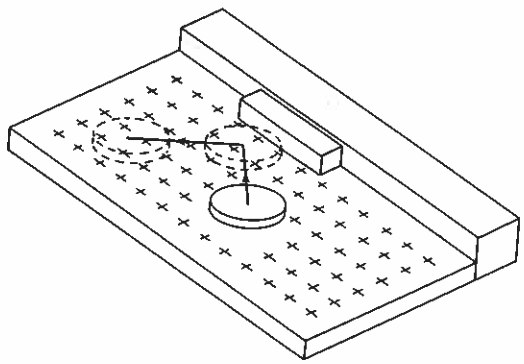

Fig. 4 Essentials of experimental apparatus

the impact time incremental changes in the tangential force become negative. Eventually these cause regions of counter-slip to be generated near to the boundary of contact. These become more dominant as the impact proceeds until, at about 90 percent of the cycle time, there are no stuck regions left and the traction $f(r) = -\mu p(r)$. It is interesting to compare these results with the appropriate curve of Fig. 1.

Trajectories. The full line in Fig. 3 shows the relation between ψ_1 and ψ_2 for the same disk as in Fig. 1. A positive angle of reflexion is one in which the tangential velocity retains the same sense. In the range $\psi_1 < 4\chi$ the simple theory, neglecting tangential elasticity, predicts $\psi_2 = 0$ corresponding to rigid body rolling at exit. When tangential elasticity is allowed for, however, negative angles of reflexion can be obtained. It is also of interest that the surfaces in contact can retain gross-slip at lower values of ψ_1 than those predicted by simple theory since tangential elastic recovery can maintain relative velocity, i.e., the surface of the half-space moves while the corresponding surface of the disk is at rest.

Experiments

A series of simple experiments was carried out in which measurements were made of the angles of incidence and reflexion of a disk impacting a fixed block. A disk shaped puck, which is a symmetrical slice cut from a sphere, is propelled toward a clamped block of similar material from which it subsequently rebounds. The puck "floats" on an air film maintained by a series of jets in a level table, Fig. 4. Virtually frictionless conditions are therefore provided.

A heavy launching device, incorporating a pendulum, provides a simple means of maintaining repeatable initial conditions. A number of adjustment facilities are provided to reset the pendulum so that a large range of incidence angles can be accommodated.

The whole experimental rig is housed in a dark room enabling the trajectory of the puck before and after impact to be photographed under stroboscopic lighting.

Three pucks were used in the experiments. Two of these were of hard steel sliced by spark erosion from commercial ball bearings, one of 3 in. diameter and the other 4 in. diameter. The material of these pucks is known to have a high coefficient of restitution and the manufacturing process by which the original spheres were formed ensured a very accurate curvature and a high quality surface finish.

Steel of matching specification was used for the impact block which was machined, hardened and polished before being clamped firmly to the air-table.

A third puck, of synthetic "rubber" was made for the purpose of testing the theory using another material. The relevant properties of the rubber, namely Poisson's ratio and the coefficient of friction, are very different from steel; in fact μ is greater than unity. Considerable attention was paid to achieving homogeneity and accuracy of shape. A casting pattern was made using the outer race of a spherical self-aligning bearing. From this a mold was cast in the same material as the puck. The surfaces of the cured mold were then coated with a thin film of petroleum jelly and the puck was vacuum cast. On setting, the puck could be removed by distorting the compliant mold. Several trial pucks were made and examined for homogeneity.

An impact block was cast in much the same way but the polished plane surface was produced by incorporating a glass slide in the mold.

The three pucks were sprayed with matt black paint on their top surface and strips of reflective tape were then applied so that the position of the puck could be highlighted at each flash of the stroboscope.

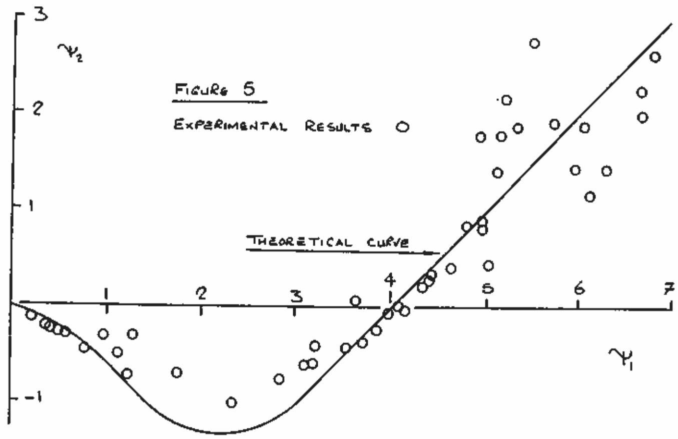

Fig. 5 Nondimensional angles of reflexion, ψ_2, plotted against nondimensional angle of incidence, ψ_1, for a "rubber" disk (ν = 0.5, χ = 1.0)

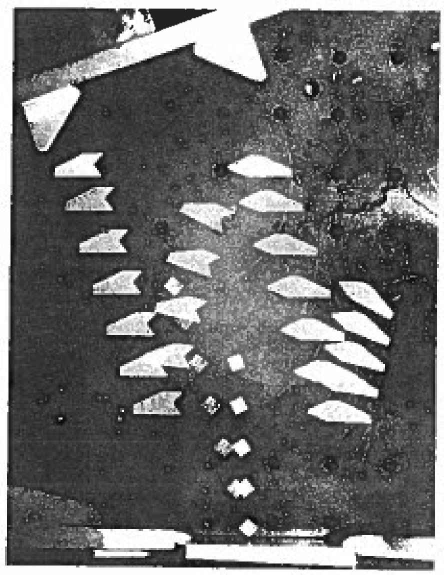

Fig. 6(a)

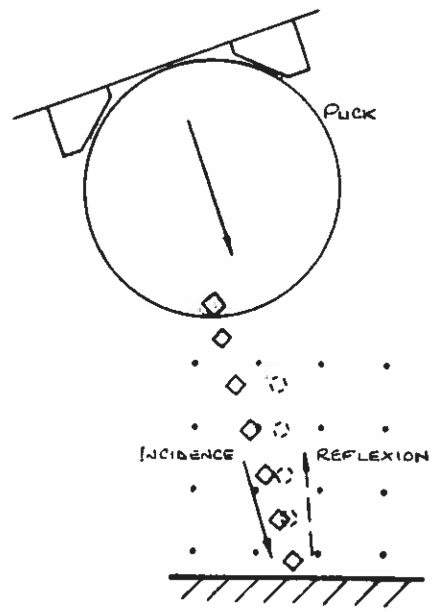

Fig. 6(b)

Fig. 6 Photographic recording and diagram of impact trajectory. Diamond shaped marker shows negative reflexion angle (about 8 deg).

Procedure. In order to relate the actual angles of incidence and reflexion to their nondimensional equivalents, values were required for μ and ν. For Poisson's ratio, values were taken from the material specification but it was necessary to measure μ. The simple and modified theories of oblique impact agree when $\psi_1 > 4\chi$ and a simple relation exists between the actual angles of incidence and reflexion and the coefficient of friction, i.e.,

$$\mu = \frac{V_{x1} - V_{x2}}{2V_{z1}\left(1 + \frac{1}{K}^2\right)} \tag{6}$$

A series of experimental values of V_{x1}/V_{z1} and V_{x2}/V_{z2} was therefore obtained by analyzing the photographic recordings of various impacts where conditions were known to be of gross-slip throughout. The photographic recordings of each impact were interpreted by transferring the highlighted locations from the print onto a sheet of plain paper via an insert of carbon paper. The plotted loci were then analyzed kinematically. Equation (6) was then used to calculate a mean value of μ. On completing the calibration a range of impacts was investigated where stick between the surfaces could be expected. The corresponding values of ψ are shown in Figs. 3 and 5.

Results for Steel Puck. Figure 3 shows experimental results for the 4 in. diameter steel puck for which the mean value of μ was 0.115. When measured using an inclined plane in conditions of dry sliding $\mu = 0.123$. However a tolerance of about $\pm$ 2 percent should be applied to the measurements so the two values are in close agreement. Results for the 3 in. diameter steel puck exhibit no new features.

In the region of gross-slip the coefficient of friction remained essentially constant ($\pm$ 5 percent of the mean value) over a wide range of ψ_1 even though the normal velocity varied and the impact durations and maximum forces therefore differed from test to test.

When $\psi_1 < 4\chi$ negative angles of reflexion were obtained demonstrating the influence of tangential elasticity when the surfaces stick during the cycle. This can be seen in Fig. 6 where the path of an additional diamond-shaped marker applied to the disk periphery can be followed before and after impact. The negative reflexion angle can be assessed if the tip of the marker is aligned with the jet lattice in the air-table. The angle measures about 8 deg.

Since ψ_1 is proportional to the local angle of incidence, a given value can be achieved by various combinations of translational and spin velocity. For instance, the puck can be aimed along a path normal to the impact, the required tangential component of velocity being provided by back-spin. Alternatively, the puck can be projected at the correct angle with no spin. If we consider the locality of the impact then, in the former case, the impact region of the half-space remains substantially at rest while, in the latter case, the disk rolls over the surface and hence the location of the contact region changes. This has practical implications in those impacts where stick occurs because it has been assumed that, at the center of the patch, the surfaces adhere both in the tangential and in the normal direction. The stresses would, presumably, tend to relieve themselves by the rolling action but the amount of rolling that occurs in a real impact is small. A typical value of 1.5 percent is obtained by comparing the tangential distance moved by the center of the disk with the maximum contact radius. However to examine this an experiment was performed in which a value of ψ_1 was selected which would excite the disk into rebounding at the maximum (negative) ψ_2. This initial condition was imposed in each of the alternative modes described above. The results from the experiments did not disclose any significant differences, though differences might occur with high forward spin and large angles of incidence.

Experimental values of ψ_2 in the partial-stick impacts were lower than predicted. It follows, therefore, that the elastic energy stored in the material was less than that expected or was not recovered to the anticipated extent. An increase in the value of μ of about 20 percent would be sufficient to restore the values of ψ_2.

The average value for the coefficient of restitution was 0.93, giving an indication of the extent to which the material behaved according to the assumptions used in the theory.

A series of experiments in which the magnitude of the approach velocity was varied by a factor of three showed that the results were independent of the approach velocity in the range considered.

Results for Rubber Puck. These are displayed in Fig. 5 and show similar trends to those of the steel puck. There is considerable scatter, however, and this increases as ψ_1 increases. This is thought to be due, in part, to drafting inaccuracy when analyzing the photographic recordings. The procedure becomes more susceptible to error as the incidence angle increases (for a given ψ_1, the actual angle of incidence was some twenty-five times that of the steel pucks). It is estimated that a tolerance band of $\pm$ 7 percent and $\pm$ 5 percent should be applied to the angles of incidence and reflexion, respectively, at values of ψ_1 in the region of 5.

The mean value of μ was 2.4 and, at the highest angles of incidence where the scatter is greatest, this has an accuracy band of about $\pm$ 25 percent. In conditions of dry sliding $\mu = 1.6$.

It is likely that the scatter is not due entirely to interpretation inaccuracy. A modified experimental procedure was used to obtain records of rebound for the rubber puck since very high angles of incidence were required to promote slip conditions. To achieve the necessary approach conditions, while at the same time retaining the advantages afforded by the launching device, the puck was subjected to two impacts. The first was used to aim the puck with back-spin at another block set to intercept it at a fine angle. At very high angles of incidence the normal velocity at the second (recorded) impact was extremely small and only slight penetration of the two surfaces would occur. It might be expected, therefore, that irregularities on the cast surfaces would have a somewhat unpredictable effect on the reflexion trajectory.

Experimental values of ψ_2 in the partial stick region were also lower than predicted. An increase in the value of μ, again of about 20 percent, would give good agreement between experiment and theory.

The average value for the coefficient of restitution was lower than that for steel at 0.86, but not sufficiently low to transgress the assumptions seriously.

Conclusions

The Hertzian theory of impact has been extended to the oblique impact of elastic bodies with Coulomb friction at the interface. It is shown, both theoretically and experimentally, that the tangential elastic compliance of the surfaces, due to frictional tractions, significantly influences the rebound angles when the local angle of incidence does not greatly exceed the angle of friction.

Acknowledgments

The authors are grateful to Professor K. L. Johnson of Cambridge University Engineering Laboratory for his advice and constructive criticism.

References

1 Hunter, S. C., "Energy Absorbed by Elastic Waves During Impact," *Journal of Mechanical and Physical Solids*, Vol. 5, 1957, pp. 162–171.

2 Lifshitz, J. M., and Kolsky, H., "Some Experiments on an Elastic Rebound," *Journal of Mechanical and Physical Solids*, Vol. 12, 1964, pp. 35–43.

3 Maw, N., Barber, J. R., and Fawcett, J. N., "The Oblique Impact of Elastic Spheres," *Wear*, Vol. 38, No. 1, 1976, pp. 101–114.

4 Maw, N., "A Theoretical and Experimental Investigation Into the Impact and Rebound of Elastic Bodies," Ph.D. thesis, C.N.A.A., Sunderland Polytechnic, England, 1976.

5 Mindlin, R. D., and Deresiewicz, H., "Elastic Spheres in Contact Under Varying Oblique Forces," ASME *Journal of Applied Mechanics*, Vol. 75, 1953, pp. 327–344.

6 Mindlin, R. D., "Compliance of Elastic Bodies in Contact," ASME *Journal of Applied Mechanics*, Vol. 71, 1949, pp. 259–268

7 Spence, D. A., "Self Similar Solutions to Adhesive Contact Problems With Incremental Loading," *Proceedings of the Royal Society*, Vol. A 305, 1968, pp. 55–80

8 Johnson, K. L., Private communication

APPENDIX

The traction distribution during gross-slip is

$$f(r) = \mu p(r) = \frac{2G\mu(b^2 - r^2)^{1/2}}{\pi R(1-\nu)}, \quad 0 \leq r \leq b$$
$$= 0 \qquad r > b$$

where b is the radius of the contact circle. It can be shown that the elastic displacement due to this traction for $r < b$ is

$$U_x(r) = \frac{\mu}{8R(1-\nu)}\left[2(2-\nu)(2b^2 - r^2) + \nu r^2 \text{ Cos } 2\theta\right]$$

in the direction of the traction; and

$$U_y(r) = \frac{\mu\nu r^2 \text{ Sin } 2\theta}{8R(1-\nu)}$$

perpendicular to the traction but in the plane of the interface.

In these expressions, the only time variant quantity is b, hence

$$V_x = \frac{d\,U_x}{dt} = \frac{\mu(2-\nu)}{R(1-\nu)}\, b\, \frac{db}{dt}$$

$$V_y = 0$$

Note that V_x is independent of r, θ. Therefore the whole contact region moves together as a rigid surface with a total velocity equal to the sliding velocity plus V_x. Consequently, when the sliding velocity is reduced to zero by the friction force, every region over the contact surface ceases to slide at the same time, i.e., the whole interface instantaneously sticks.